

## ON THE CONSTITUTIVE MODELING OF THE HOT DEFORMATION BEHAVIOR OF A HIGH-Mn TWINNING-INDUCED PLASTICITY STEEL

Hongshuang Di, Jingqi Zhang, Xiaoyu Wang

State Key Laboratory of Rolling and Automation, Northeastern University; Heping Qu, Wenhua Street; Shenyang, Liaoning 110004, P.R. China

Keywords: Constitutive modeling, Hot deformation, Twinning-induced plasticity steel

### Abstract

The hyperbolic-sine model is commonly used to describe the constitutive relation between the strain rate, temperature and the peak or steady-state stress. However, for the purpose of modeling of the hot deformation behavior, the strain should be taken into consideration. In this study, the hot deformation behavior of a high-Mn twinning-induced plasticity steel was studied by using isothermal compression tests conducted in the temperature range of 900 to 1150 °C and strain rate range of 0.001 to 20 s<sup>-1</sup>. Based on the hyperbolic-sine model, the constitutive equations of the steel were developed by using the flow stress data. The strain was introduced in the constitutive equations through the material constants  $\alpha$ ,  $n$ ,  $Q$  and  $A$ . Comparison of the flow stresses based on the constitutive equations with those obtained from the tests suggests that the developed constitutive equations can give a precise modeling of the hot deformation behavior of the steel investigated.

### Introduction

Constitutive equations are of great importance in modeling the hot forming processes, such as rolling, forging and extrusion. Over the past decades, various models have been proposed to describe the relationship between stress and strain rate for the high temperature steady state deformation. Garofalo [1] has suggested a famous empirical hyperbolic-sine model to cover the dependence of steady state creep rate on stress at constant temperatures for both high and low stresses:

$$\dot{\epsilon} = A [\sinh(\alpha\sigma)]^n \quad (1)$$

where  $A$  is material constant,  $\alpha$  is stress multiplier and  $n$  is stress exponent. Subsequently, on the basis of Garofalo's equation, Sellars and Tegart [2] have introduced another empirical hyperbolic-sine relationship to correlate the stress, strain rate and temperature under hot working conditions:

$$Z = \dot{\epsilon} \exp(Q/RT) = A [\sinh(\alpha\sigma)]^n \quad (2)$$

where  $Z = \dot{\epsilon} \exp(Q/RT)$  is the Zener-Hollomon parameter and  $Q$  is the apparent activation energy. If  $\alpha\sigma < 0.8$  (low stress), the difference between  $\sinh(\alpha\sigma)$  and  $\alpha\sigma$  is less than 10% so that Eq. (2) can be approximated by a power-law relationship which has proved quite successful for describing the creep behavior:

$$Z = A' \sigma^n \quad (3)$$

Similarly, for  $\alpha\sigma > 1.2$  (high stresses), the difference between  $\sinh(\alpha\sigma)$  and  $e^{\alpha\sigma}/2$  is less than 10%. Eq. (2) can be approximated by an exponential-law relationship:

$$Z = A'' \exp(\beta\sigma) \quad (4)$$

In Eqs. (3) and (4)  $A'$ ,  $A''$  and  $\beta$  are material constants. It should be noted that Eq. (2) (Sellars-Tegart-Garofalo equation) is normally used to characterize steady state flow stress which is independent of strain. The strain, which is an important parameter for hot deformation, has not been considered in the equation. However, for the purpose of modeling of hot deformation behavior, it is important to develop constitutive equations which characterize the material behavior taking account of all the processing parameters (i.e. strain rate, temperature and strain).

Sellars-Tegart-Garofalo equation contains four material constants ( $\alpha$ ,  $n$ ,  $Q$  and  $A$ ) which need to be determined. Several methods have been reviewed by Rieiro et al. [3] for the determination of the parameters. Generally, a suitable value for  $\alpha$  has to be introduced before  $n$ ,  $Q$  and  $A$  can be determined. A common approach is to calculate the value of  $\alpha$  according to the following relation [4-6]:

$$\alpha = \frac{\beta}{n'} \quad (5)$$

where  $\beta = (\partial \ln \dot{\epsilon} / \partial \sigma)_T$  can be determined by linear regression of Eq. (4) and  $n' = (\partial \ln \dot{\epsilon} / \partial \ln \sigma)_T$  can be obtained by linear regression of Eq. (3). Another widely-used method for determining  $\alpha$  is to force fit the flow stress data by plotting  $\ln[\sinh(\alpha\sigma)]$  vs.  $\ln \dot{\epsilon}$  for different  $\alpha$  values [4]. The value that results in the parallelism between the  $\ln[\sinh(\alpha\sigma)]$  vs.  $\ln \dot{\epsilon}$  plots should be selected.

In the previous study, the former method (Eq. (5)) has been employed to derive the constitutive equations of a high-Mn twinning-induced plasticity steel [7]. It has been shown that the developed constitutive equations could give a very good prediction of experimental data. The main purpose of the present work is to develop the strain-dependent constitutive equations of the same steel by using the latter method. Comparison was also made between the two methods on the materials constants and the prediction accuracy of the established constitutive equations.

### Materials and experimental procedures

The steel for this study were sampled from industrial rolling slabs which had been hot rolled. The composition of the steel is as follows: 23.04 wt.% Mn, 1.86 wt.% Al, 0.19 wt.% C, 0.15 wt.% Si, 0.07 wt.% V, 0.016 wt.% P, 0.002 wt.% S and balance Fe.

Cylindrical compression specimens measuring 10 mm in diameter and 15 mm in height were machined by electrodischarge machining (EDM) from the as-received steel. In order to reduce the friction between the contacting surfaces of the specimens and the dies, MoS<sub>2</sub>-coated Ta foil was inserted between the specimen and the die. A thermocouple was welded at the middle of specimen length to provide an accurate temperature control and measurement during testing. Hot compression tests were conducted on a Gleeble-3500 thermo-mechanical simulator in the temperature range of 9000 to 1150 °C (with an interval of 50 °C) for the constant strain rates of 0.001 s<sup>-1</sup>, 0.01 s<sup>-1</sup>, 0.1 s<sup>-1</sup>, 1 s<sup>-1</sup>, 10 s<sup>-1</sup> and 20 s<sup>-1</sup>. The specimens were heated to 1200 °C at the rate of 20 °C/s, homogenized at that temperature for 180 s, cooled at a rate of 5 °C/s to the selected test temperature and held for 30 s before compression. All the specimens were deformed to a true strain of about 0.9 and immediately water quenched after the test was finished.

During the test, a problem arises, particularly at high strain rates, as a result of internal heat generation. High strain rates can lead to the rapid internal generation of heat which cannot be dissipated quickly because of the short deformation time, causing significant increases in temperature of the specimen. The temperature rise due to deformation heating is usually

estimated using the following relation:

$$\Delta T = \frac{0.95\eta}{\rho C_p} \int_0^\epsilon \sigma d\epsilon \quad (6)$$

where  $\rho$  is the material density,  $C_p$  is the specific heat and  $\eta$  is the thermal efficiency.

It is also worth noting that the use of MoS2-coated Ta foil can reduce friction but will never eliminate it completely. There is still some friction as all the tested specimens displayed a small level of barreling. Since the friction can influence the flow stress, it is important for the levels of friction to be quantified. Details of correcting both deformation heating and friction have been given in a previous paper [7].

## Results and discussion

### Determination of materials constants

Taking logarithm of both sides of Eq. (2) yields:

$$\frac{1}{n} \ln \dot{\epsilon} + \frac{Q}{nRT} - \frac{\ln A}{n} = \ln(\sinh(\alpha\sigma)) \quad (7)$$

It is noted from Eq. (7) that at a given strain the experimental data should yield linear and parallel  $\ln[\sinh(\alpha\sigma)]$  vs.  $\ln \dot{\epsilon}$  plots for different temperatures. In the  $\sinh(\alpha\sigma)$  analysis, the value of  $\alpha$  was taken from similar alloys, as reported in the literature [6,8-12]. It was decided to vary from 0.0070 to 0.0150  $\text{MPa}^{-1}$ . The  $\alpha$  which makes the slopes of  $\ln[\sinh(\alpha\sigma)]$  vs.  $\ln \dot{\epsilon}$  plots become almost equal was selected as the appropriate value. The value of  $n$  was calculated from the average of the slopes of  $\ln[\sinh(\alpha\sigma)]$  vs.  $\ln \dot{\epsilon}$  plots.

By partial differentiation of Eq. (2), the apparent activation energy for deformation  $Q$  can be obtained as:

$$Q = 10000R \left\{ \frac{\partial \ln \dot{\epsilon}}{\partial \ln[\sinh(\alpha\sigma)]} \right\}_T \left\{ \frac{\partial \ln[\sinh(\alpha\sigma)]}{\partial (10000/T)} \right\}_\dot{\epsilon} \quad (8)$$

or

$$Q = 10000Rn \left\{ \frac{\partial \ln[\sinh(\alpha\sigma)]}{\partial (10000/T)} \right\}_\dot{\epsilon} \quad (9)$$

Taking natural logarithm on of both sides of Eq. (2) gives:

$$\ln Z = \ln A + n \ln[\sinh(\alpha\sigma)] \quad (10)$$

The  $\ln Z$  vs.  $\ln[\sinh(\alpha\sigma)]$  plot can be used for obtaining the value of  $\ln A$ .

Fig. 1 shows the example of determination of the materials constants in Sellars-Tegart-Garofalo equation for the investigated steel at a strain of 0.5. The values of  $\alpha$ ,  $n$ ,  $Q$  and  $\ln A$  at a strain of 0.5 were determined to be 0.0082  $\text{MPa}^{-1}$ , 4.7930, 372.59 kJ/mol and 31.65, respectively. Following the same procedure, the values of  $\alpha$ ,  $n$ ,  $Q$  and  $\ln A$  at any strain level in the range of 0.1 to 0.7 with an interval of 0.05 can be obtained.

Fig. 2 shows the variations in the materials constants with strain. For purpose of comparison, the values that were calculated by the former method as discussed in the introduction were also shown in the figure. As compared to those reported in the previous work, the values of  $\alpha$  do not show significant variation with strain. Similar result was also obtained by Phaniraj et al. [13]. Conversely, the values of  $n$  exhibit a shaper decrease with the increase of strain, varying in a wide range of 4.6220 to 7.0746. Nevertheless, those values are comparable to those reported for

austenitic steels [9-12]. Referring to Fig. 2c, the activation energy  $Q$  decreases with increasing strain. The values obtained by the two methods do not show significant difference. Li et al. [12] reported a value of 387.84 kJ/mol for an austenitic Fe-20Mn-3Si-3Al transformation induced plasticity steel; Hamada et al. [14] determined a value of 377 kJ/mol for Fe-25Mn twinning-induced plasticity steel; Xiong et al. [15] reported a value of 439 kJ/mol for Fe-23Mn-0.6C high-Mn steel. The values obtained in the present work are close to those reported in the literature.

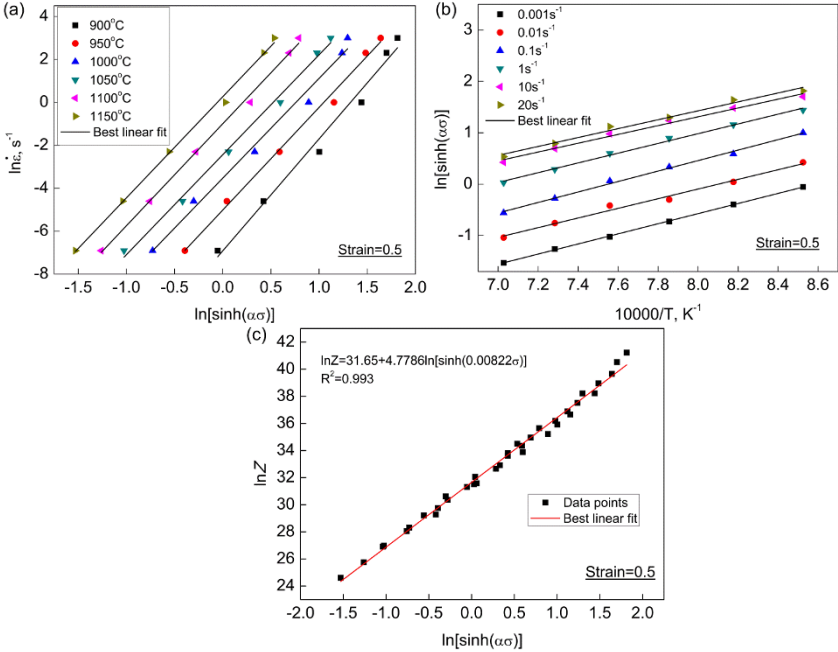


**Fig. 1.** Relationships between (a)  $\ln \dot{\epsilon}$  and  $\ln[\sinh(\alpha\sigma)]$ ; (b)  $\ln[\sinh(\alpha\sigma)]$  and  $10000/T$  and  $\ln Z$  and  $\ln[\sinh(\alpha\sigma)]$

In the present work, it is found that a 5<sup>th</sup> order polynomial, as given by Eq. (11), is capable of describing the variation of material constants with strain with very good correlation and generalization:

$$\begin{cases} \alpha = -0.0173\epsilon^5 + 0.0900\epsilon^4 - 0.1389\epsilon^3 + 0.0910\epsilon^2 - 0.0259\epsilon + 0.0107 \\ n = -19.714\epsilon^5 + 61.383\epsilon^4 - 77.237\epsilon^3 + 53.524\epsilon^2 - 21.915\epsilon + 8.8009 \\ Q = 4714.0\epsilon^5 - 10562\epsilon^4 + 8866.6\epsilon^3 - 3205.0\epsilon^2 + 306.67\epsilon + 424.32 \\ \ln A = 399.76\epsilon^5 - 906.65\epsilon^4 + 769.16\epsilon^3 - 279.99\epsilon^2 + 27.008\epsilon + 36.111 \end{cases} \quad (11)$$

Once the values of materials constants were determined, the flow stress at any temperature, strain rate and strain can be obtained according to the following equations.

$$\begin{cases} \sigma = \frac{1}{\alpha} \ln \left\{ (Z/A)^{1/n} + \left[ (Z/A)^{2/n} + 1 \right]^{1/2} \right\} \\ Z = \dot{\epsilon} \exp(Q/RT) \end{cases} \quad (12)$$

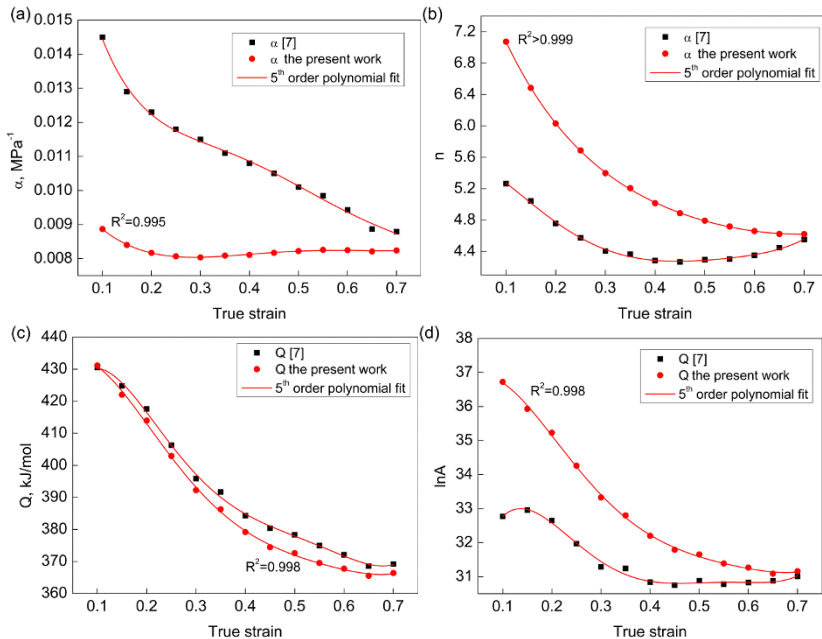


**Fig. 2.** Variation of (a)  $\alpha$ , (b)  $n$ , (c)  $Q$  and (d)  $\ln A$  with strain.

### Verification of the developed constitutive equations

Fig. 3 shows the comparisons between the experimental data and the flow stresses calculated by the constitutive equations, together with those reported in Ref. [7]. It clearly demonstrates that the calculated flow stresses have very good agreement with the experimental value. To determine how accurately the developed constitutive equations describe the experimental data, an error analysis was also performed in terms of correlation coefficient ( $R$ ) and average absolute relative error ( $AARE$ ), which are respectively expressed as:

$$R = \frac{\sum_{i=1}^N (E_i - \bar{E})(C_i - \bar{C})}{\sqrt{\sum_{i=1}^N (E_i - \bar{E})^2 \sum_{i=1}^N (C_i - \bar{C})^2}} \quad (13)$$

and

$$AARE(\%) = \frac{1}{N} \sum_{i=1}^N \left| \frac{E_i - C_i}{E_i} \right| \times 100 \quad (14)$$

where  $E$  is the experimental data and  $C$  is the calculated value by the developed constitutive equations,  $\bar{E}$  and  $\bar{C}$  are the mean values of  $E$  and  $C$ , respectively,  $N$  is the number of data. As shown in Fig. 4, the value of  $R$  was found to be 0.999, which demonstrates a very good correlation between the experimental and the calculated data. The value of  $AARE$  was obtained as 2.85%. In the previous study by the former method [7], the values of  $R$  and  $AARE$  were determined to be 0.996 and 3.31%. These statistical analyses suggest both the constitutive equations developed by the two methods can give an accurate estimate for high temperature flow

stress of the steel investigated; the constitutive equations developed by the latter method show a better prediction of the experimental data than those by the latter.

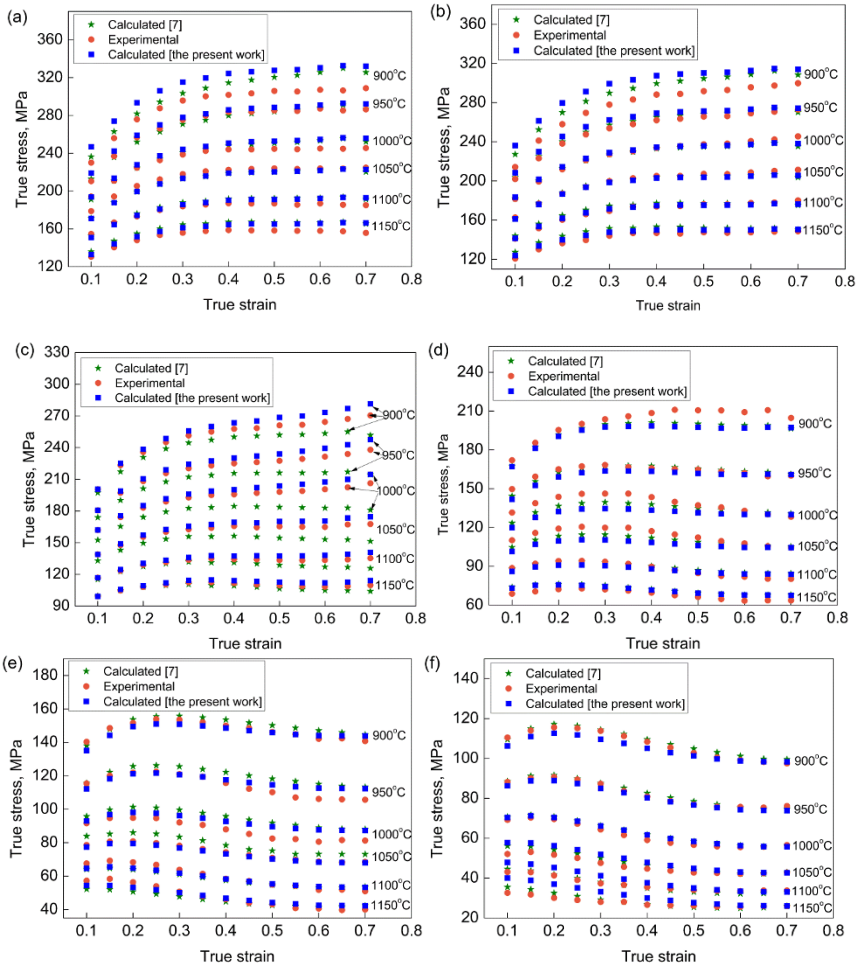


**Fig. 3.** Comparison of the experimental and calculated flow stresses by the two methods at different strain rates: (a)  $20 \text{ s}^{-1}$ , (b)  $10 \text{ s}^{-1}$ , (c)  $1 \text{ s}^{-1}$ , (d)  $0.1 \text{ s}^{-1}$ , (e)  $0.01 \text{ s}^{-1}$  and (f)  $0.001 \text{ s}^{-1}$ .

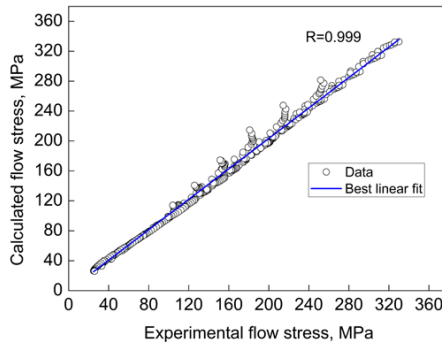


**Fig. 4.** Correlation between the experimental and calculated flow stresses by the developed constitutive equations.

### Conclusions

1. The constitutive equations of a high-Mn twinning-induced plasticity steel were derived on the basis of Sellars-Tegart-Garofalo equation. The influence of strain on the hot deformation behavior of the steel was incorporated in the constitutive equations by considering the effect of strain on material constants.
2. The material constants ( $\alpha$ ,  $n$ ,  $Q$  and  $\ln A$ ) were found to be functions of the strain. A 5<sup>th</sup> order polynomial was found to represent the influence of strain on material constants with very good correlation and generalization.
3. Comparison between the calculated and experimental results shows that they are in good agreement. The prediction accuracy of the strain-compensated constitutive equations was further quantified in terms of correlation coefficient ( $R$ ) and average absolute relative error ( $AARE$ ). The value of  $R$  and  $AARE$  was found to be 0.999 and 2.85% respectively. The results suggest the developed constitutive equation is valid and accurate.

### Acknowledgements

This work was financially supported by the National Program on Key Basic Research Project (No. 2011CB606306-2) and Fundamental Research Funds for the Central Universities (No. N110607005).

### References

1. F. Garofalo, *Fundamentals of creep and creep-rupture in metals* (New York, NY: Macmillan, 1965), 50-54
2. C.M. Sellars and W.J. McG. Tegart, "On the mechanism of hot deformation," *Acta Materialia*, 14(1966), 1136-1138.
3. I. Rieiro, V. Gutiérrez, J. Castellanos, M. Carsí, M.T. Larrea, and O.A. Ruano, "A new constitutive strain-dependent Garofalo equation to describe the high-temperature processing of materials-application to the AZ31 magnesium alloy," *Metallurgical and Materials Transactions A*, 41(2010), 2396-2407.
4. H.J. McQueen and N.D. Ryan, "Constitutive analysis in hot working," *Materials Science and Engineering: A*, 322(2002), 43-63.

5. Y.C. Lin, M.S. Chen, and J. Zhong, "Constitutive modeling for elevated temperature flow behavior of 42CrMo steel," *Computational Materials Science*, 42(2008), 470-477.
6. S. Mandal, V. Rakesh, P.V. Sivaprasad, S. Venugopal, and K.V. Kasiviswanathan, "Constitutive equations to predict high temperature flow stress in a Ti-modified austenitic stainless steel," *Materials Science and Engineering: A*, 500(2009), 114-121.
7. J.Q. Zhang, H.S. Di, X.Y. Wang, Y. Cao, J.C. Zhang, and T.J. Ma, "Constitutive analysis of the hot deformation behavior of Fe-23Mn-2Al-0.2C twinning induced plasticity steel in consideration of strain," *Materials & Design*, 44(2013), 354-364.
8. H. Mirzadeh, J.M. Cabrera, and A. Najafizadeh, "Modeling and prediction of hot deformation flow curves," *Metallurgical and Materials Transactions A*, 43(2012), 108-123.
9. B.F. Guo, H.P. Ji, X.G. Liu, L. Gao, R.M. Dong, M. Jin, and Q.H. Zhang, "Research on flow stress during hot deformation process and processing map for 316LN austenitic stainless steel," *Journal of Materials Engineering and Performance*, 21(2011), 1455-1461.
10. H. Yuan and W.C. Liu, "Effect of the  $\delta$  phase on the hot deformation behavior of Inconel 718," *Materials Science and Engineering: A*, 528(2005), 281-289.
11. C.Y. Sun, J.R. Liu, R. Li, and Q.D. Zhang, "Constitutive modeling for elevated temperature flow behavior of Incoloy 800H superalloy," *Acta Metallurgica Sinica*, 47(2011), 191-196.
12. D.J. Li, Y.R. Feng, Z.F. Yin, F.S. Shangguan, K. Wang, Q. Liu, and F. Hu, "Hot deformation behavior of an austenitic Fe-20Mn-3Si-3Al transformation induced plasticity steel," *Materials & Design*, 34(2012), 713-718.
13. C. Phaniraj, Dipti Samantaray, Sumantra Mandal, and A.K. Bhaduri, "A new relationship between the stress multipliers of Garofalo equation for constitutive analysis of hot deformation in modified 9Cr-1Mo (P91) steel," *Materials Science and Engineering: A*, 528(2011:528), 6066-6071.
14. A.S. Hamada, L.P. Karjalainen, and M.C. Somani, "The influence of aluminum on hot deformation behavior and tensile properties of high-Mn TWIP steels," *Materials Science and Engineering: A*, 467(2007), 114-124.
15. W. Xiong, B. Wietbrock, A. Saeed-Akbari, M. Bambach, and G. Hirt, "Modeling the flow behavior of a high-Manganese steel Fe-Mn23-C0.6 in consideration of dynamic recrystallization," *Steel Research International*, 82(2011), 127-136.